Materials Research Bulletin 47 (2012) 2277–2281

Contents lists available at SciVerse ScienceDirect

Materials Research Bulletin

journal homepage: www.elsevier.com/locate/matresbu

Synthesis of vertically aligned boron nitride nanosheets using CVD method

Chao Zhang, Xiaopeng Hao *, Yongzhong Wu *, Miao Du

State Key Laboratory of Crystal Materials, Shandong University, 27 Shandanan Road, Jinan 250100, PR China

ARTICLE INFO

Article history:
Received 23 October 2011
Received in revised form 27 April 2012
Accepted 23 May 2012
Available online 6 June 2012

Keywords:
A. Nitrides
B. Vapor deposition
D. Optical properties
D. Luminescence

ABSTRACT

Boron nitride nanosheets (BNNSs) protruding from boron nitride (BN) films were synthesized on silicon substrates by chemical vapor deposition technique from a gas mixture of BCl_3–NH_3–H_2–N_2. Parts of the as-grown nanosheets were vertically aligned on the BN films. The morphology and structure of the synthesized BNNSs were characterized by scanning electron microscopy, transmission electron microscopy, and Fourier transformation infrared spectroscopy. The chemical composition was studied by energy dispersive spectroscopy and X-ray photoelectron spectroscopy. Cathodoluminescence spectra revealed that the product emitted strong UV light with a broad band ranging from 250 to 400 nm. Field-emission characteristic of the product shows a low turn-on field of 6.5 V μm^{-1}.

1. Introduction

Recently, 2D materials have attracted great attention since the appearance of the graphene which has been found to possess excellent quantum transport and mechanical properties [1]. Hexagonal boron nitride is comprised of layered structures as the isoelectric analog of graphite. Compared with graphite carbon, BN has excellent mechanical properties and thermal conductivity and is much more thermally and chemically stable, which makes BN a better candidate for composite materials in hazardous environments [2,3]. Boron nitride is a semiconductor with a wide band gap near 6 eV, in contrast to the semimetallic nature of graphite. Recent researches have revealed that BN is of high promise in application of ultraviolet (UV) light emission devices [4,5]. As the main member of BN nanomaterials, single or few layers of boron nitride have interesting properties and potential applications. Terrones et al. found that BN nanoribbons with zigzag edges can behave as metals, thus exhibiting excellent electron field emission properties [6]. Yu et al. detected that boron nitride nanosheets were superhydrophobicity [5]. Ultrathin BN nanosheets protruding from BN fibers and ultrathin BN nanosheets protruding from Si_3N_4 nanowires had been found to exhibit excellent field emission properties [7,8].

Up to now, several methods have been proposed to obtain graphene analogs of boron nitride, including micromechanical cleavage a bulk BN crystal [9], unwrapping multiwalled BN nanotubes through plasma etching [10], sonication [11,12] of BN particles or using a high-energy electron beam [13,14], solid phase reaction [15] and chemical vapor deposition [16,17]. Vertically aligned boron nitride nanosheets were prepared on silicon substrates from gas mixture of BF_3–N_2–H_2 through microwave plasma chemical vapor deposition (MPCVD) technique previously. Yu et al. proposed that the etchant of F atoms and the electrical field were the main reasons for the formation of vertically aligned BNNSs [5].

In this paper, we report the synthesis of 2D boron nitride nanosheets protruding from BN films on silicon substrates from gas mixture of BCl_3–NH_3–H_2–N_2 by chemical vapor deposition technique. No electrical field was applied. The structure and morphology of the products were systematically investigated by scanning electron microscopy, transmission electron microscopy and Fourier transformation infrared spectroscopy. The chemical composition was studied by energy dispersive spectroscopy and X-ray photoelectron spectroscopy. The optical property of boron nitride nanosheets studied via cathodoluminescence spectra reveals strong cathodoluminescence emission in the ultraviolet range, and this indicates that the present novel BN nanosheets are highly promising for application in optical devices. A turn-on electric field of 6.5 V μm^{-1} has been observed in the as-prepared BN nanosheets.

2. Experimental

The growth of the BNNSs protruding from BN films was performed in a quartz tube type conventional CVD system. A silicon monocrystal wafer as the substrate was placed in the center of the quartz tube. The furnace was first flushed with pure nitrogen gas for 30 min and then the furnace was heated under

---

* Corresponding authors. Tel.: +86 0531 88366218; fax: +86 0531 88362321.
E-mail addresses: xphao@sdu.edu.cn (X. Hao), wuyz@sdu.edu.cn (Y. Wu).

0025-5408/$ – see front matter © 2012 Elsevier Ltd. All rights reserved.
http://dx.doi.org/10.1016/j.materresbull.2012.05.042

N_2 + 5% H_2 gas (200 ml min^{-1}). When the temperature of the substrate reached 1000 °C, NH_3 and BCl_3 were separately introduced into the tube. The gas flow rates of N_2 + 5% H_2, BCl_3, NH_3 were 200, 15, 150 ml min^{-1}, respectively. After 30 min, the gases BCl_3 and NH_3 were cut off and the furnace cooled down to ambient temperature.

The morphology and structure were examined by a Hitachi S-4800 scan electron microscopy (SEM) and a JEOL JEM-2100 high-resolution transmission electron microscopy (HRTEM) operated at 200 kV. Fourier transform infrared (FTIR) spectroscopic study was carried out on a NEXUS 670 FT-IR. Chemical composition was determined using an energy dispersive spectroscopy (EDS) system attached to S-4800 SEM and an ESCALAB 250 X-ray photoelectron spectroscopy (XPS). A cathodoluminescence (CL) spectrophotometer attached to a SU-70 field emission scan electron microscopy (FE-SEM) was used to investigate optical properties of the synthesized product. The field emission (FE) property of the product was measured in a vacuum chamber, which was pumped down to 10^{-6} Pa by an ultrahigh vacuum system.

3. Results and discussion

The SEM images of the obtained sample are shown in Fig. 1a and b. The substrate surface is homogeneously covered by a thick

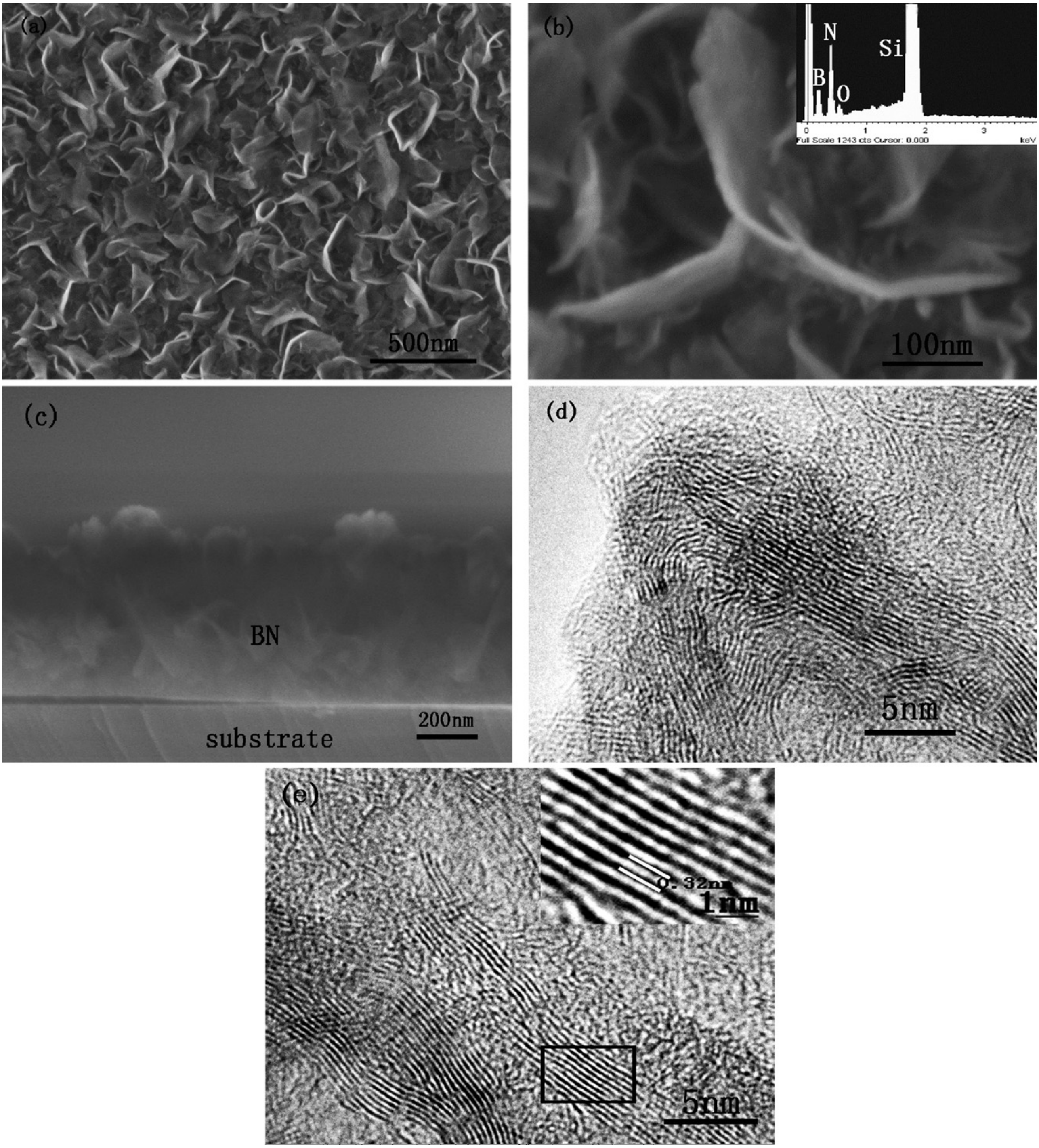

Fig. 1. (a) Low and (b) high magnification SEM images of the product (the inset is the EDS spectrum of the product); (c) section SEM image; (d) and (e) HRTEM images of the product (the inset is the enlarged image of the rectangle domain).

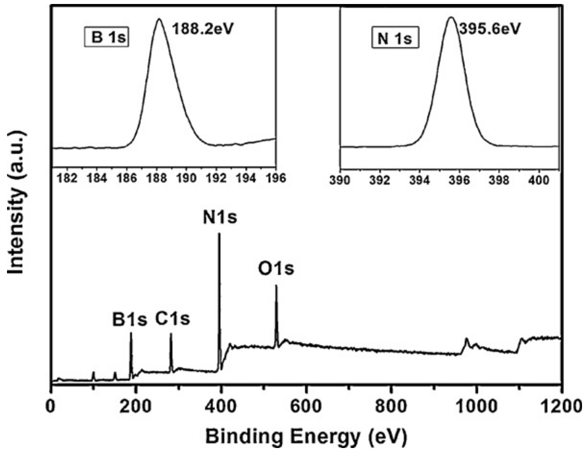

Fig. 2. Wide scan, B 1s (inset: upper left) and N 1s (inset: upper right) XPS spectra recorded from the product.

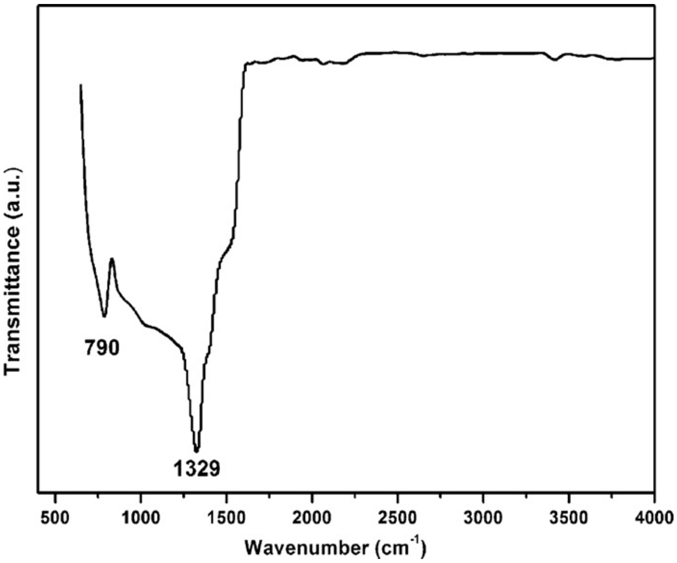

Fig. 3. FTIR spectrum of the product.

layer of nanosheets, as shown in Fig. 1a. The high-magnification image (Fig. 1b) shows that parts of the nanosheets are vertically aligned on the substrate. The thickness of the aligned nanosheets is less than 10 nm. The inset image in Fig. 1b shows the chemical composition of the product. The elements of B, N, Si and O can be found from the spectrum. The Si signal comes from the silicon substrate, and the weak O signal comes from the oxidation of the silicon substrate during the heating process. Fig. 1c is the section image of the product. It can be found that the BNNSs protruding from boron nitride films not directly protruding from the silicon substrate.

Fig. 1d and e shows the typical HRTEM images of the synthesized BNNSs, which reveal that the BNNSs have a graphite analogs structure. The banding structure can be detected only when the edge of the BNNSs turned up. From the turned up edges,

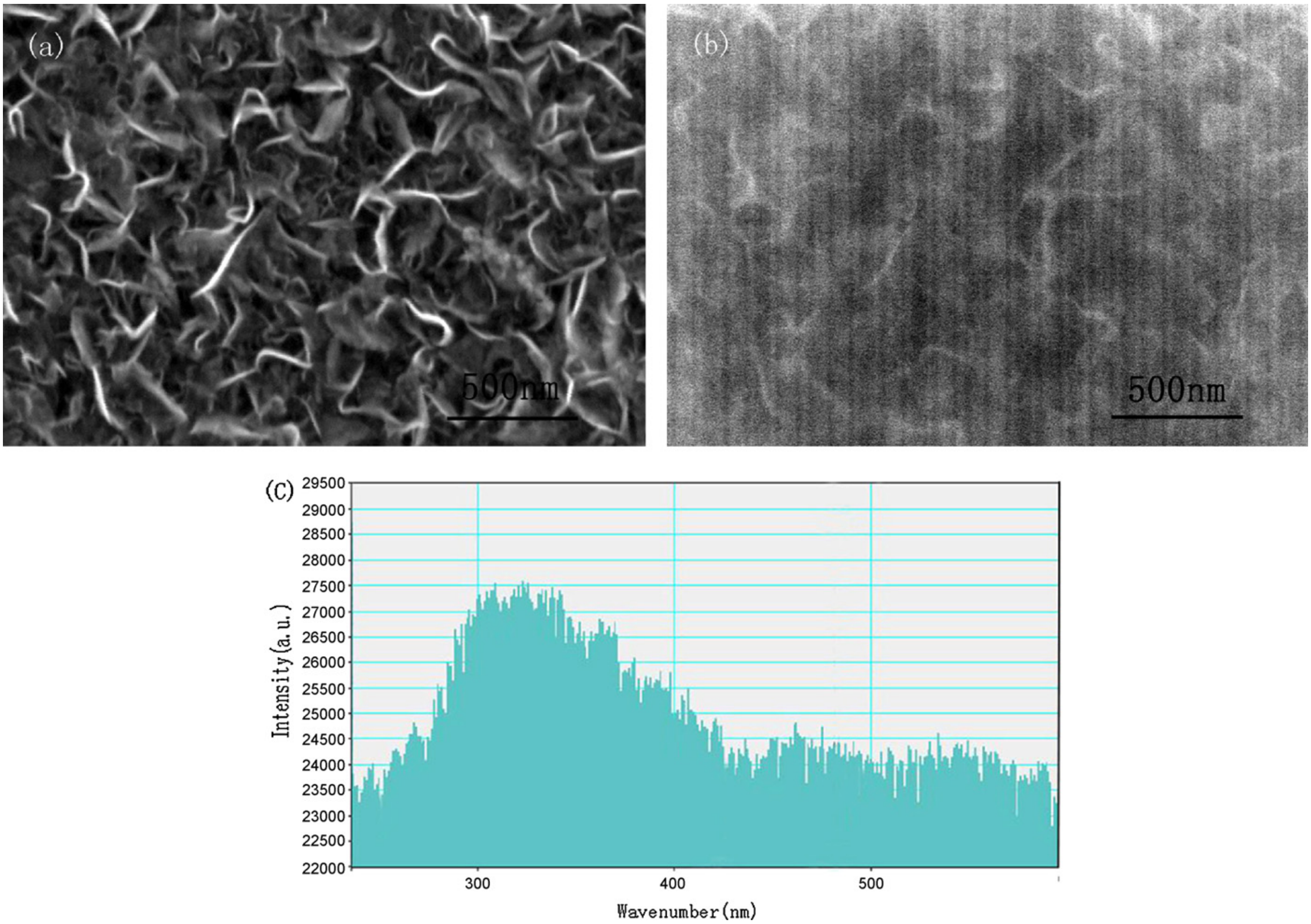

Fig. 4. (a) SEM image of the product; (b) CL image from the corresponding (a); (c) CL spectrum from the product.

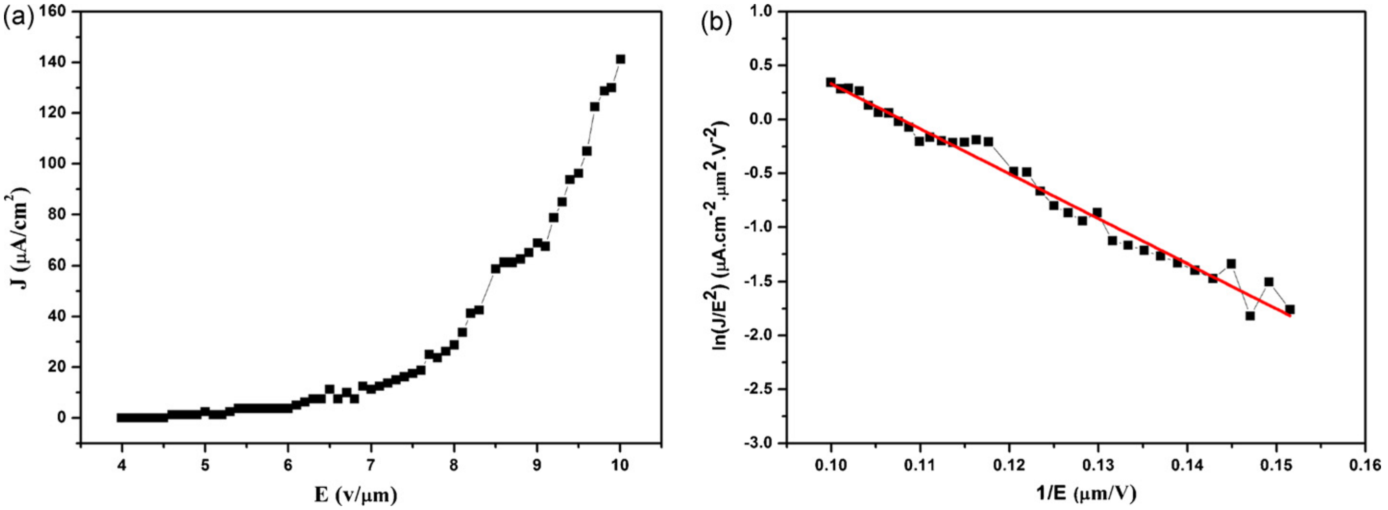

Fig. 5. FE properties of the BNNSs protruding from BN films: (a) *J*–*E* curve; (b) a Fouler–Nordheim plot corresponding to (a), and the straight line is a linear fit of the $\ln(J/E^2) - (1/E)$ plot.

it can be found that the thickness of the nanosheets is less than 10 nm, consisting with the SEM images. The inset in Fig. 1e is the enlarged image of the rectangle domain, where highly ordered lattice fringes can be clearly observed. The interplane spacing is about 0.32 nm, corresponding to the (0 0 2) plane of the hexagonal system of BN.

The chemical composition of the product was also studied by XPS. The peaks of elements Si, C, O, B, and N can be observed on the survey spectrum, as shown in Fig. 2. The intensity of Si signal is very weak, which comes from the silicon substrate. The elements of C and O come from the CO_2, O_2, or H_2O adsorbed on the surface of the BNNSs. The high-resolution B 1s and N 1s spectra are displayed in the insets of Fig. 2. The binding energies centered at 188.2 eV for B 1s and 395.6 eV for N 1s are found from it, which are consistent with the reported values [18]. The atomic ratio of B–N is about 0.98:1 through the quantification of the B 1s and N 1s peaks (S.F.: B, 0.159; N, 0.477), which is in good agreement with the BN stoichiometry.

The synthesized BNNSs were further examined using FTIR. Fig. 3 shows the FTIR spectrum of the product. There are two strong vibrations at 790 and 1329 cm^{-1}, which can be ascribed to the A2u (B–N–B bending vibration mode parallel to the *c*-axis) and E1u (B–N stretching vibration mode perpendicular to the *c*-axis) modes of h-BN, respectively [19]. The weak absorption peak near 3410 cm^{-1} can be attributed to the O–H bonds owing to the water absorbed on the product surface.

CL was applied to measure the optical properties of the prepared BNNSs. Fig. 4a and b depicts the SEM and CL luminescence images of the product, respectively. Fig. 4c is a typical CL spectrum of the synthesized BNNSs. It can be seen that a broad emission band centered around 320 nm in the range of 250–420 nm. The near band edge CL luminescence emission is not observed from the present CL spectrum. The strong ultraviolet CL emission from BNNSs can be attributed to the deep-level emissions associated with defect-related centers (B or N vacancy-type defect-trapped states) [17,19]. This strong ultraviolet emission indicated that the product is highly promising for application in optical devices.

Fig. 5a shows the plot of the FE current density (J) as a function of the applied field (E) for the product. The turn-on field is determined to be 6.5 V μm^{-1} at a current density of 10 μA cm^{-2}. Fig. 5b displays the corresponding Fowler–Nordheim (FN) plot, $\ln(I/E^2) = -52(B\Phi^{3/2}/\beta)E^{-1} + \ln(A\alpha\beta^2/\Phi)$, where I is the current density, E is the applied field ($E = V/d$), Φ is the work function, β is the field-enhancement factor, B and A are constants, and α is the effective emission area. The plot of $\ln(I/E^2)$ versus E^{-1} gives an approximately straight line, and this confirms that the field emission is consistent with the conventional FN theory.

A possible reaction mechanism for the boron nitride nanosheets is proposed here. The reaction occurs in this process can be expressed as follows: $BCl_3 + NH_3 \rightarrow BN + 3HCl$. With a series of experiments, we find that the flow rate of BCl_3 is crucial to the formation of nanosheets. When the flow rate of BCl_3 is low, only a thick layer of particles is formed. So we think that the growth rate will become faster with the density of BCl_3 increasing, especially in domain containing defects. Meanwhile new BN species, upon landing on the surface of a growing BNNS, quickly moved along the surface toward the edge of the nanosheet and covalently bonded to the edge atoms with high mobility. Thus, the BNNSs tended to grow higher rather than thicker.

4. Conclusions

BNNSs protruding from BN films have been successfully synthesized using a simple CVD technique. Parts of the BNNSs are vertically aligned on the BN films with a graphite analogs structure. The thickness of the BNNSs is less than 10 nm. A strong cathodoluminescence emission in the ultraviolet range was detected from the product, and this indicates that the BNNSs are highly promising for application in optical devices. The FE characteristic of the product shows a low turn-on field of 6.5 V μm^{-1}.

Acknowledgements

This work was financially supported by National Basic Research Program of China (2009CB930503), NSFC (Contract Nos. 50801042, 50823009), the Fund for the Natural Science of Shandong Province (ZR2010EM020, ZR2010EM049), and SRF for ROCS, SEM.

References

[1] K.S. Novoselov, A.K. Geim, S.V. Morosov, D. Jiang, Y. Zhang, S.V. Dubonos, I.V. Grigorieva, A.A. Firsov, Science 306 (2004) 666–669.
[2] J.J. Pouch, A. Alterovitz, Synthesis and Properties of Boron Nitride, vol. 54–55, Trans Tech Publications, Zürich, 1990.
[3] C. Zhi, Y. Bando, C. Tang, D. Golberg, Mater. Sci. Eng. Res. 70 (2010) 92–111.
[4] K. Watanabe, T. Taniguchi, H. Kanda, Nat. Mater. 3 (2004) 404–409.
[5] J. Yu, L. Qin, Y. Hao, S. Kuang, X. Bai, Y.-M. Chong, W. Zhang, E. Wang, ACS Nano 4 (1) (2010) 414–422.

[6] M. Terrones, J.-C. Charlier, A. Gloter, E. Cruz-Silva, E. Terrés, Y.B. Li, A. Vinu, Z. Zanolli, J.M. Dominguez, H. Terrones, Y. Bando, D. Golberg, Nano Lett. 8 (4) (2008) 1026–1032.
[7] Z.-G. Chen, J. Zou, J. Mater. Chem. 21 (2011) 1191–1195.
[8] Y. Zhu, Y. Bando, L. Yin, D. Golberg, Nano Lett. 6 (12) (2006) 2982–2986.
[9] D. Pacilé, J.C. Meyer, Ç.Ö. Girit, A. Zettl, Appl. Phys. Lett. 92 (2008) 133107.
[10] H. Zeng, C. Zhi, Z. Zhang, X. Wei, X. Wang, W. Guo, Y. Bando, D. Golberg, Nano Lett. 10 (12) (2010) 5049–5055.
[11] C. Zhi, Y. Bando, C. Tang, H. Kuwahara, D. Golberg, Adv. Mater. 21 (2009) 2889–2893.
[12] W.-Q. Han, L. Wu, Y. Zhu, K. Watanabe, T. Taniguchi, Appl. Phys. Lett. 93 (2008) 223103.
[13] J.C. Meyer, A. Chuvilin, G. Algara-Siller, J. Biskupek, U. Kaiser, Nano Lett. 9 (7) (2009) 2683–2689.
[14] C. Jin, F. Lin, K. Suenaga, S. Iijima, Phys. Rev. Lett. 102 (2009) 195505.
[15] A. Nag, K. Raidongia, K.P.S.S. Hembram, R. Datta, U.V. Waghmare, C.N.R. Rao, ACS Nano 4 (3) (2010) 1539–1544.
[16] A. Pakdel, C. Zhi, Y. Bando, T. Nakayama, D. Golberg, ACS Nano 5 (2011) 6507–6515.
[17] R. Gao, L. Yin, C. Wang, Y. Qi, N. Lun, L. Zhang, Y.-X. Liu, L. Kang, X. Wang, J. Phys. Chem. C 113 (2009) 15160–15165.
[18] Q. Guo, Y. Xie, C. Yi, L. Zhu, P. Gao, J. Solid State Chem. 178 (2005) 1925–1928.
[19] C. Zhi, Y. Bando, C. Tang, D. Golberg, R. Xie, T. Sekigushi, Appl. Phys. Lett. 86 (2005) 213110.